Laser Cooling of a Solid by 16 K Starting from Room Temperature

C. E. Mungan,* M. I. Buchwald, B. C. Edwards, R. I. Epstein, and T. R. Gosnell†
Los Alamos National Laboratory, Mail Stop E543, Los Alamos, New Mexico 87545
(Received 16 September 1996)

An Yb^{3+}-doped optical fiber is laser cooled *in vacuo* from 298 to 282 K. Cooling results from anti-Stokes fluorescence of the ytterbium ions after optical pumping at a wavelength of 1015 nm. The sample temperature is deduced from the emission spectrum, which is sensitive to the populations in the excited-state multiplet of the ions. The temperature change is limited by the coupling between the fiber and ambient blackbody radiation, as confirmed when samples suddenly exposed to the pump laser are found to exponentially relax towards thermal steady state with the expected time constants. [S0031-9007(97)02372-7]

PACS numbers: 32.80.Pj, 42.81.–i, 44.60.+k, 78.55.Hx

It is well known that free atoms can be translationally cooled by scattering photons that are Doppler shifted into resonance with an atomic absorption. On average, the isotropically emitted photons have higher energy than the input photons—the difference equals the heat loss. Since its first description in 1975 [1], laser cooling of gas-phase atoms has steadily progressed and recently culminated in demonstrations of Bose-Einstein condensation of the atomic ensemble [2]. Less well known is an analogous idea, proposed much earlier [3–5], that is applicable to the luminescent cooling of gases as well as *condensed* phases: When optical pumping is used to induce departures from the quasiequilibrium populations in two radiatively coupled energy-level manifolds, cooling results if the relaxation from the upper to the lower manifold is purely radiative and if the emitted photons have larger mean energy than the absorbed photons. For instance, suppose that the lower manifold consists of a single level and the upper manifold consists of two levels spaced by a few kT. Optical pumping from the ground level to the lowest level of the upper manifold will cool the sample, provided that the intermanifold decay is radiative yet slower than the intramanifold thermalization. While such an anti-Stokes cooling mechanism has been observed for a gas [6] and more recently for a liquid [7–9], the only previously reported attempt to demonstrate photoluminescent cooling of a solid prior to a year ago yielded merely reduced sample heating [10]. Last year, however, net cooling of a solid—an Yb^{3+}-doped glass—was demonstrated for the first time [11]. While this result served as a proof of principle, the actual measured temperature drop was small—only 0.3 K.

In this Letter, we present the results of cooling experiments on Yb^{3+}-doped glass in a sample geometry favorable for large net cooling, namely, that of an optical-fiber waveguide. The sample temperature is determined by measuring its laser-induced fluorescence spectrum. Temperature drops of up to 16 K starting from RT are observed, in agreement with predictions based on the assumption that the dominant heat load on the samples is background blackbody radiation.

Clad cylindrical preforms of the fluorozirconate glass ZBLANP (ZrF_4-BaF_2-LaF_3-AlF_3-NaF-PbF_2), suitable for drawing into optical fibers, were cast. The cores of these fibers were doped with 1 wt % Yb^{3+} and comprised ~70% of the total diameter of the samples. The undoped ZBLAN cladding has a refractive index at 1.0 μm, ~1% lower than the 1.52 index of the core [12], thus yielding fibers with numerical apertures of ~0.2. After testing the cores for cooling by photothermal deflection spectroscopy [11], the preforms were drawn into multimode fibers having outer diameters between 135 and 400 μm. No protective coatings were applied to the fibers during manufacture.

For each series of measurements, an ~2-cm-long piece of fiber is cleaved, examined under a microscope, and immediately inserted into a vacuum chamber. To minimize the conductive heat load from the surroundings, the fiber is horizontally supported by two thin vertical glass slides and the chamber is evacuated to 10^{-5} torr. The interior walls of the chamber are painted black to avoid reflecting the emitted light. Silica glass windows transmit the pump laser light into the fiber and permit collection of the fluorescence emitted at 90° to the fiber axis from a volume of the fiber about midway between its two ends.

The output beam from a cw titanium-sapphire laser is focused to a spot diameter of ~50 μm and centered on one of the fiber faces. Sample fluorescence is collected from a few-mm-long section of the fiber with a collimating lens and focused with a second lens onto the entrance slit of a 1-m monochromator. A right-angle periscope between the two lenses is used to flip the line image of the fiber from horizontal to vertical. The signal beam is chopped at 50 Hz and lock-in detected using a thermoelectrically cooled InGaAs photodiode. Both the pump laser and the monochromator can be tuned from 850 to 1100 nm, spanning the entire RT absorption and fluorescence spectra of the $^2F_{7/2} \rightarrow {}^2F_{5/2}$ Yb^{3+} transition [11]. The slit width corresponds to a spectral resolution of 0.8 nm, considerably finer than the ~8-nm linewidth of the sharpest spectral feature, namely, the prominent 0-0

 0031-9007/97/78(6)/1030(4)$10.00

peak at 975 nm. The emission spectra are corrected for the responsivity of the detection optics and electronics, as measured using a standard lamp.

In order to calibrate the fluorescence-based temperature measurements, reference emission spectra near RT are obtained by filling the vacuum chamber with ~1 atm of He gas, either cooling or heating the entire chamber, and measuring the temperatures using a thermocouple. The laser pump is reduced to low power and is tuned to the wavelength corresponding to the mean energy of the emitted photons, so that neither optical heating nor cooling should occur. Two examples of reference spectra, obtained at temperatures of 290 and 303 K, are shown in Fig. 1(a). For both spectra, the 0-0 peak intensity has been normalized to unity for ease of comparison. The shapes of the two curves are visibly different—the inset plot shows the arithmetic difference between the high- and low-temperature normalized spectra.

To observe laser cooling of the fiber (or heating, depending on the pump wavelength), the vacuum chamber is evacuated and the temperature changes of the fiber are measured as follows. For any given laser wavelength, fluorescence spectra are collected at both high and low laser powers. (Thermal drift of the sample during the monochromator scans can be neglected because of the fiber's small heat capacity and strong radiative coupling to the massive vacuum chamber—see the discussion of Fig. 3 below). The high- and low-power spectra are normalized and subtracted in the manner of Fig. 1(a). As an example, Fig. 1(b) shows normalized spectra obtained for a 250-μm-diameter fiber pumped at 1015 nm. The corresponding difference spectrum is plotted in the inset. The temperature change of the sample, ΔT, is obtained by comparing the areas of the resulting difference spectra with the reference difference spectrum of Fig. 1(a). Since the temperature changes of the sample are small enough to be directly proportional to the amplitudes of these difference spectra, calculation of a linear scale factor accurately determines ΔT [13]. The signal-to-noise ratio in the inset difference spectrum in Fig. 1(a) is good enough to resolve temperature changes down to at least 1 K.

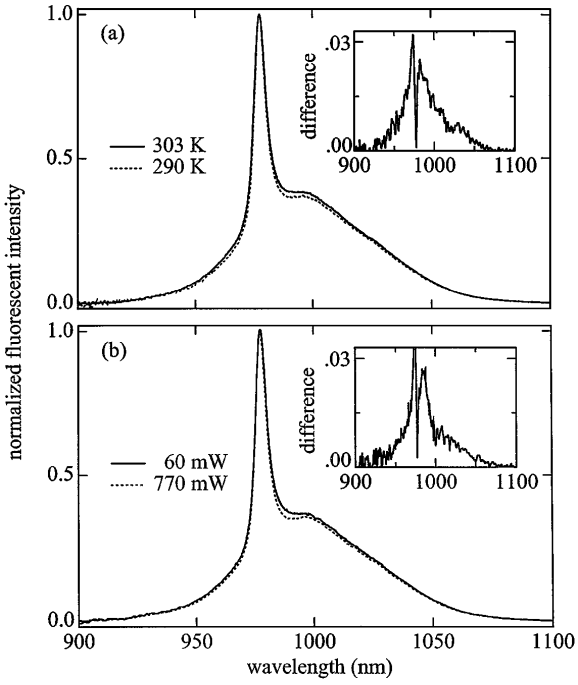

FIG. 1. (a) Fluorescence spectra, normalized to the intensity of the 0-0 peak, for the indicated fiber temperatures. The scattered laser peaks, which have a resolution-limited FWHM of ~1 nm, have been subtracted off. Inset: Difference between the high- and low-temperature spectra from the main part of the figure. (b) Analogous data obtained for low and high power laser pumping of the fiber *in vacuo*. Comparison of the difference data shown in the inset with that of panel (a) indicates a laser-induced temperature drop of 16 K.

In order to compare temperature changes for different pump wavelengths, ΔT is normalized by the difference ΔP between the high and low laser powers used, where each value of the power is reduced by the factor $\exp(-\alpha L/2)$ [14]. Here α is the absorption coefficient of ZBLANP +1 wt% Yb^{3+} at the laser wavelength and $L/2$ is the distance from the input face to the sampled volume of the fiber. The laser power is kept low enough at all wavelengths that the intensity of the light within the fiber's core was never more than 10% of the corresponding saturation intensity [15].

All of the fibers exhibit laser cooling at long wavelengths. The largest temperature drop occurs for a pump wavelength of 1015 nm in all cases. Specifically, the power-normalized temperature changes at this wavelength are 11 K/W for a fiber of 400-μm total diameter and 26 K/W for a 250-μm fiber. (These values are found to vary by up to 40% for different pieces of fiber taken from the same spool, presumably due to heating effects from surface contamination of bulk imperfections.) As expected [cf. Eq. (1) below], the normalized temperature change is inversely proportional to the fiber diameter, to within the experimental uncertainties. On the other hand, a 135-μm fiber exhibits a temperature drop of only 15 K/W, which is much less than the expected 40 K/W, suggesting that impurities have been introduced during the manufacturing.

Our best results for a $D \equiv 250$-μm diameter fiber are plotted as the filled circles in Fig. 2. Panel (a) presents $\Delta T/\Delta P$ as a function of the pump wavelength. Cooling is observed for wavelengths longer than 1005 nm. The largest temperature drop is 16 K starting from RT, observed upon increasing the laser power at 1015 nm from 60 to 770 mW. Temperature changes can be converted to cooling efficiencies η_R relative to the absorbed laser power P_{abs} by way of the expression

$$\eta_R \equiv \frac{P_{\mathrm{cool}}}{P_{\mathrm{abs}}} \cong \frac{4\pi D\sigma T_R^3 \Delta T}{\alpha \Delta P}, \qquad (1)$$

where σ is the Stefan-Boltzmann constant and T_R is room temperature (namely, 298 K during a typical run). This

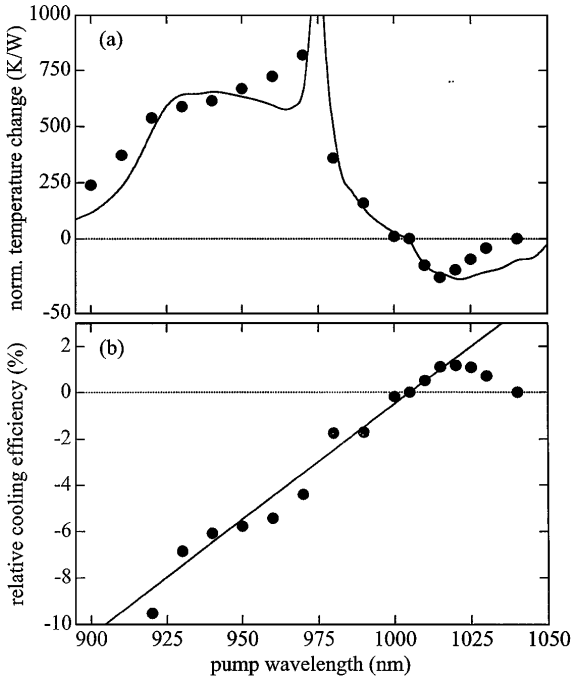

FIG. 2. (a) Measured temperature changes (filled circles) of a 250-μm diameter fiber, normalized by the laser power at the midpoint of the sample. The continuous curve is derived from Eq. (1) using the theoretical cooling powers expected if $\lambda_F^* = 1005$ nm. Note the change in the vertical scale at 0 K/W. (b) The cooling efficiencies (filled circles), relative to the absorbed laser power, calculated from the observed temperature changes. The straight line is a plot of $(\lambda - 1005\ \text{nm})/1005\ \text{nm}$.

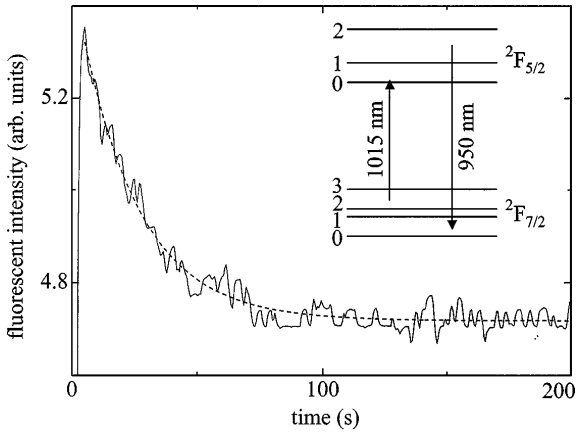

FIG. 3. Fluorescence signal (solid curve) measured at 950 nm after suddenly unblocking the pump laser (having a power of 790 mW and a wavelength of 1015 nm) at time $t = 0$. The dashed curve is the best fit to a single exponential with a time constant of 24 s. Inset: Energy-level diagram (not to scale) of ZBLANP:Yb^{3+} with the pump and monitored emission photon energies indicated schematically.

relation assumes that the cooling power P_{cool} is equal to the blackbody radiative heat load from the RT walls of the chamber. Using this equation, cooling efficiencies can be calculated from the data of Fig. 2(a); these results are plotted in Fig. 2(b).

Measuring the time required for the fiber temperature to settle after suddenly unblocking the pump laser confirms that the dominant heat load on the fiber is radiative. The solid curve in Fig. 3 shows the fluorescence intensity collected at 950 nm for a pump wavelength of 1015 nm, as sketched in the inset level diagram. The laser is unblocked at time $t = 0$. (The finite rise time of the signal reflects the 300-ms time constant of the lock-in amplifier.) The subsequent drop in signal amplitude is due to the decreasing temperature of the fiber which results, in turn, from the reduced intensity of both the short-wavelength fluorescence (due to diminished population in the high-lying levels of the $^2F_{5/2}$ excited-state manifold) and the long-wavelength absorption (due to decreased population in the high-lying levels of the $^2F_{7/2}$ ground-state manifold). The dashed curve in the figure is the best fit of the data to a single exponential, with a relaxation time constant of (24 ± 3) s. Similarly, exponential relaxation of the temperature of a 400-μm diameter fiber, with a fitted time constant of (39 ± 4) s is obtained, when it is heated by laser pumping at 930 nm and the fluorescence intensity is measured at 975 nm. For this choice of wavelengths, the absorption and fluorescence strengths both decline as the fiber warms up. Radiative coupling with the surroundings is expected to result in exponential thermal relaxation with a time constant of $C/(4\pi DL\sigma T_R^3)$, since the emissivity of ZBLANP is approximately unity of the wavelength range of a RT blackbody. Here πDL is the surface area of the fiber and $C = c_m \rho \pi D^2 L/4$ is its heat capacity, since its volume is $\pi D^2 L/4$. Approximating the physical properties of ZBLANP by those of ZBLA, the specific heat c_m is 0.53 $\text{J g}^{-1}\,\text{K}^{-1}$ and the density ρ is 4.54 g cm^{-3} [12]. Thus the time constants are predicted to be $c_m \rho D/(16\sigma T_R^3) = 25$ s for the 250-μm diameter fiber and 40 s for the 400-μm fiber, independent of the fiber lengths. These calculated values are in excellent agreement with the observed time constants.

The above results demonstrate two independent facts: First, the ions must reach thermal equilibrium with the host glass on a time scale small compared with the 1.9-ms lifetime of the excited-state multiplet [15]. More significantly, the time-dependent spectral changes are in excellent accord with a purely thermal model—for two different fiber diameters—and therefore any nonthermal spectral effects arising from ion-ion interactions or other microscopic phenomena are not significant enough to corrupt the temperature measurement. This validates the fluorescence thermometry technique used here. As a further check on this conclusion, the fluorescence spectra of both a fiber pumped at low laser powers and a bulk sample pumped at high powers were measured (at constant temperature) and their shapes were found to be reproducible and independent of pump wavelength to better than 0.5%.

In general, the optical cooling power can be shown by energy conservation to be $P_{\text{cool}} = P_{\text{abs}}(\lambda - \lambda_F^*)/\lambda_F^*$,

where λ is the pump wavelength and $\lambda_F^* \equiv \lambda_F/\eta$. Here λ_F is the wavelength corresponding to the mean energy of the emitted photons that escape from the fiber and η is the quantum efficiency for photon emission and escape. The mean-emission energy is found by computing the first moment of the Yb^{3+} fluorescence spectrum in the frequency domain. For the 250-μm-diameter fiber, λ_F at RT is found to be (995 ± 2) nm. As a function of wavelength, the relative cooling efficiency would thus be expected to map out a straight line crossing zero at 995 nm if η were exactly unity. In contrast, the data in Fig. 2(b) cross zero at 1005 nm; the continuous curves plotted in both panels are the expected efficiencies and power-normalized temperature changes for $\lambda_F^* = 1005$ nm. This indicates that $\eta = 0.99$, i.e., 1% of the absorbed laser light is converted entirely into heat. This might arise from absorption of the fluorescence by surface impurities introduced in the course of pulling the fibers. Furthermore, in Fig. 2(b), the data points fall below the straight line at the longest and shortest wavelengths. This may arise from spurious heating effects due to broadband absorption of the pump light directly by nonfluorescing species such as Fe^{2+}, Cu^{2+}, and OH^- [16]. Finally, the systematic curvature in the experimental data near the 0-0 peak frequency of 975 nm might arise from uncertainties in the values of α.

In summary, laser cooling of Yb^{3+}-doped optical fibers is observed. The sample temperatures are determined nonintrusively by collecting photoinduced fluorescence spectra and interpolating their intensity profiles between those measured independently at known temperatures. Temperature drops as large as 16 K are observed, demonstrating that the results reported in Ref. [11] scale in the expected manner. The measured temperature changes agree well with the values calculated under the assumption that the dominant heat load is radiative, if the quantum efficiency is taken to be 0.99. The samples exponentially relax towards thermal steady state with expected time constants, confirming that radiative coupling to the environment dominates the cooling dynamics.

We would like to thank J. C. Fajardo for stimulating interactions. This work has been carried out under the auspices of the U.S. Department of Energy.

*Present address: Dept. of Physics, University of West Florida, Pensacola, FL 32514-5751.

†Author to whom correspondence should be addressed. Electronic address: <gosnell@lanl.gov>

[1] T. W. Hänsch and A. L. Schawlow, Opt. Commun. **13**, 68 (1975).

[2] M. H. Anderson *et al.*, Science **269**, 198 (1995); K. B. Davis *et al.*, Phys. Rev. Lett. **75**, 3969 (1995); C. C. Bradley, C. A. Sackett, and R. G. Hulet (to be published).

[3] P. Pringsheim, Z. Phys. **57**, 739 (1929).

[4] L. Landau, J. Phys. (Moscow) **10**, 503 (1946).

[5] A. Kastler, J. Phys. Radium **11**, 255 (1950).

[6] N. Djeu and W. T. Whitney, Phys. Rev. Lett. **46**, 236 (1981).

[7] C. Zander and K. H. Drexhage, in *Advances in Photochemistry*, edited by D. C. Neckers, D. H. Volman, and G. von Bünau (Wiley, New York, 1995), p. 59.

[8] J. L. Clark and G. Rumbles, Phys. Rev. Lett. **76**, 2037 (1996).

[9] C. E. Mungan and T. R. Gosnell, Phys. Rev. Lett. **77**, 2840 (1996).

[10] T. Kushida and J. E. Geusic, Phys. Rev. Lett. **21**, 1172 (1968).

[11] R. I. Epstein, M. I. Buchwald, B. C. Edwards, T. R. Gosnell, and C. E. Mungan, Nature (London) **377**, 500 (1995).

[12] M. Poulain, in *Fluoride Glass Fiber Optics*, edited by I. D. Aggarwal and G. Lu (Academic, San Diego, 1991), p. 1.

[13] In particular, reference spectra collected at 293 and 298 K were found to interpolate linearly between the 290 and 303 K spectra.

[14] In the absence of thermal diffusion, the attenuation of the laser power along the length of the fiber gives rise to a temperature distribution, since the local temperature change is proportional to the local pump power. A 1D model shows that, for the small departures from RT in our experiment, thermal diffusion does not significantly modify this temperature distribution near the midpoint of the fiber, even for wavelengths near the 975-nm absorption peak.

[15] X. Zou and H. Toratini, Phys. Rev. B **52**, 15 889 (1995).

[16] S. Mitachi, Y. Terunuma, Y. Ohishi, and S. Takahashi, J. Lightwave Technol. **2**, 587 (1984).